Association of the 1q25 diabetes-specific coronary heart disease locus with alterations of the γ-glutamyl cycle and increased methylglyoxal levels in endothelial cells.

Caterina Pipino[1,2,3], Hetal Shah[1,2], Sabrina Prudente[4], Natalia Di Pietro[3], Lixia Zeng[5], Kyoungmin Park[1,2], Vincenzo Trischitta[6,7], Subramanian Pennathur[5], Assunta Pandolfi[3], Alessandro Doria[1,2]

1. Research Division, Joslin Diabetes Center, Boston, MA, USA
2. Department of Medicine, Harvard Medical School, Boston, MA, USA
3. Department of Medical, Oral and Biotechnological Sciences, Center for Advanced Studies and Technology - CAST (ex CeSI-MeT), University G. d'Annunzio of Chieti-Pescara, Chieti, Italy
4. Research Unit of Metabolic and Cardiovascular Diseases, Fondazione IRCCS Casa Sollievo della Sofferenza, San Giovanni Rotondo, Italy.
5. Division of Nephrology, Department of Medicine, University of Michigan
6. Research Unit of Diabetes and Endocrine Diseases, Fondazione IRCCS Casa Sollievo della Sofferenza, San Giovanni Rotondo, Italy.
7. Department of Experimental Medicine, Sapienza University, Rome, Italy.

Corresponding Author:
Dr. Alessandro Doria,
Joslin Diabetes Center
One Joslin Place,
Boston, MA 02215
Phone: 617-309-2406
Email: alessandro.doria@joslin.harvard.edu

Word Count: Abstract: 200, Main text: 4,492, Figures/tables: 6/0

ABSTRACT

A chromosome 1q25 variant (rs10911021) has been associated with coronary heart disease (CHD) in type 2 diabetes (T2D). In human umbilical vein endothelial cells (HUVECs), the risk allele 'C' is associated with lower expression of the adjacent gene *GLUL* encoding glutamine synthase, converting glutamic acid to glutamine. To further investigate the mechanisms through which this locus affects CHD risk, we measured 35 intracellular metabolites involved in glutamic acid metabolism and γ–glutamyl cycle in 62 HUVEC strains carrying different rs10911021 genotypes. Eight metabolites were positively associated with the risk allele (17%-58% increase/allele copy, p=0.046-0.002), including five γ–glutamyl amino acids, β-citryl-glutamate, N-acetyl-aspartyl-glutamate, and ophthalmate - a marker of γ–glutamyl cycle malfunction. Consistent with these findings, the risk allele was also associated with decreased glutathione/glutamate ratio (-9%, p=0.012), decreased S-lactoylglutathione (-41%, p=0.019), and reduced detoxification of the atherogenic compound methylglyoxal (+54%, p=0.008). *GLUL* down-regulation by shRNA caused a 40% increase in methylglyoxal level, which was completely prevented by glutamine supplementation. In summary, we have identified intracellular metabolic traits associated with the 1q25 risk allele in HUVECs, including impairments of the γ–glutamyl cycle and methylglyoxal detoxification. Glutamine supplementation abolishes the latter abnormality, suggesting that such treatment may prevent CHD in 1q25 risk allele carriers.

INTRODUCTION

Despite improvements in glycemic control and other preventive therapies, individuals with type 2 diabetes continue to experience an increased burden of cardiovascular complications such as coronary heart disease (CHD) (1). In order to change the status quo, new interventions are needed that specifically target the mechanisms linking the diabetic milieu to vascular damage. Our strategy to gain insights into these mechanisms, and identify novel targets for preventive therapies, has been to study the genetic factors that modulate cardiovascular risk among persons with type 2 diabetes (2).

Following this approach, we have discovered a locus on chromosome 1q25 that was associated with CHD, with genome-wide significance, in multiple sets of patients with type 2 diabetes (3). Subsequent studies have confirmed this finding in other populations with type 2 diabetes (4; 5). This CHD locus is placed in the region of the *GLUL* gene, which codes for glutamate-ammonia ligase (also known as glutamine synthase) catalyzing the conversion of glutamic acid to glutamine (6). In the original report, the risk allele of the lead variant (rs10911021) was associated with decreased *GLUL* expression in endothelial cells and with a lower pyroglutamic-to-glutamic acid ratio in plasma, suggesting an impairment of glutamic acid metabolism and the γ-glutamyl cycle, of which pyroglutamic acid is an intermediate, as a possible mechanism underlying the association with CHD (3). The γ-glutamyl cycle is responsible for the generation of glutathione – a natural anti-oxidant playing a critical role in the protection from free radicals and other reactive compounds (7), whose deficit may predispose to increased oxidative stress and accelerated atherosclerosis (7; 8).

The goal of the present study was to seek further support for this hypothesis by analyzing the association at the cellular level between the 1q25 lead variant (rs10911021) and metabolites involved in glutamic acid metabolism and the γ-glutamyl cycle in a unique collection of human umbilical vein endothelial cells (HUVECs) isolated from a large group of newborns and therefore allowing the study of the impact of natural genetic variation on cellular functions. Our results support the hypothesis of an

association between 1q25 locus and γ-glutamyl cycle alterations, and point to a reduced glutathione-mediated detoxification of methylglyoxal - a precursor of advanced glycation end-products (AGE) - as a possible mechanism linking these metabolic changes to the increased CHD risk experienced by 1q25 risk allele carriers with type 2 diabetes.

RESEARCH DESIGN AND METHODS

HUVEC preparation and culture

The study was carried out on HUVECs isolated from the umbilical cords of 62 newborns delivered by randomly selected, healthy Caucasian mothers between the 36th and the 40th gestational week at the Hospital of Chieti and Pescara (Italy). HUVECs were isolated from the umbilical cords by extraction with 1 mg/mL collagenase 1A at 37°C, as previously described (9). All procedures were in agreement with the ethical standards of the local Institutional Committee on Human Experimentation (reference number: 1879/09COET) and with the Declaration of Helsinki Principles. After approval of the protocol by the Institutional Review Board, signed informed consent was obtained from each participating subject.

For this study, HUVECs were grown on 1.5% gelatin-coated tissue culture plates (Sigma-Aldrich) in complete low-glucose (1 g/L) culture medium composed of Dulbecco's modified Eagle's medium (DMEM; provided by Joslin Media Core) supplemented with 20% fetal bovine serum (FBS, Gibco by life technologies), 200 U/mL penicillin, 200 µg/mL streptomycin (Sigma-Aldrich), 10 µg/mL heparin (Stem Cell Technologies) and 50 µg/mL endothelial cells growth factor (ECGF; Alpha Aeser). HUVECs were maintained in incubator at 37°C and in humidified atmosphere of 5% CO_2/95% air and sub-cultured using 0.05% trypsin/0.02% ethylenediaminetetraacetic acid (EDTA). Cells between the 3rd and 7th passages were used in all experiments.

Genotyping

DNA was extracted from HUVECs by standard methods. Genotyping of the rs10911021 variant was performed by means of a custom TaqMan assay (Life Technologies, Foster City, CA) on a 7900HT platform (Applied Biosystems, Foster City, CA). Genotyping quality was tested by including six blinded duplicate samples in each 96-well assay. The average agreement rate of duplicate samples was greater than 99%.

Metabolomic profiling

Cell culture: HUVECs at 60-70% confluence were incubated with media containing 10% FBS and 5.5 mM D-glucose (basal condition, low glucose) or 25 mM D-glucose (high glucose). Following 48 hours of treatment, cells were trypsinized, transferred to a 50 mL polypropylene Falcon tube, and centrifuged at 1,200 rpm for 10 minutes. Supernatants were discarded and cell pellets gently re-suspended in phosphate buffer saline (PBS) and transferred to pre-labeled 2.0 mL polypropylene tubes. Cell suspensions were centrifuged (1,200 rpm for 10 minutes) and all supernatants carefully removed. Cell pellets were immediately stored at -80°C until all biological replicates were collected, and shipped to Metabolon (Durham, NC, USA) for metabolomic profiling.

Metabolite measurements: The present study considered 35 metabolites involved in glutamic acid metabolism, the γ-glutamyl cycle, and glutathione metabolism that were extracted from a larger Metabolon panel of 597 metabolites according to the pre-specified hypothesis of an impact of the 1q25 locus on these metabolic pathways. These 35 metabolites included all those whose "Sub –pathway" field in the Metabolon report was labeled as "Glutathione metabolism" (n=9), "Glutamate Metabolism" (n=13), or "γ-Glutamyl Amino Acid" (n=10), plus cysteine and glycine (the two amino acids that are used together with glutamic acid to synthesize glutathione) and alpha-ketoglutarate – a Krebs cycle intermediate that is in direct equilibrium with glutamic acid through amination/deamination by glutamate dehydrogenase. Samples were prepared by Metabolon using the automated MicroLab STAR® system from Hamilton Company. Several recovery standards were added prior to the first step in the

extraction process for quality control purposes. To remove proteins, dissociate small molecules bound to proteins or trapped in the precipitated protein matrix, and to recover chemically diverse metabolites, proteins were precipitated with methanol under vigorous shaking for 2 min (Glen Mills GenoGrinder 2000) followed by centrifugation. The resulting extracts were divided into five fractions: two for analysis by two separate reverse phase (RP)/UPLC-MS/MS methods with positive ion mode electrospray ionization (ESI), one for analysis by RP/UPLC-MS/MS with negative ion mode ESI, one for analysis by HILIC/UPLC-MS/MS with negative ion mode ESI, and one reserved for backup. Samples were placed briefly on a TurboVap® (Zymark) to remove the organic solvent. Extracts were stored overnight under nitrogen before preparation for analysis.

Quality Assurance (QA)/Quality Control (QC): Several types of controls were analyzed along with the experimental samples: a pooled matrix sample generated by taking a small volume of each experimental sample served as a technical replicate throughout the analyses; extracted water samples served as process blanks; and a cocktail of QC standards spiked into every analyzed sample allowed for instrument performance monitoring and aided chromatographic alignment. Instrument variability was determined by calculating the median relative standard deviation (RSD) for the standards that were added to each sample prior to injection into the mass spectrometers. Overall process variability was determined by calculating the median RSD for all endogenous metabolites (i.e., non-instrument standards) present in 100% of the pooled matrix samples. Experimental samples were randomized across the platform run with QC samples spaced evenly among the injections.

Western blotting

When 70% confluence was reached, HUVECs were cultured in basal conditions (5.5 mM D-glucose) or treated with high glucose (25 mM D-glucose) for 48 hours. Briefly, cells were washed with cold PBS and `lysed in RIPA buffer (Sigma Aldrich), with the addition of protease and phosphatse inhibitors (cat. P8340 and cat. P5726, Sigma Aldrich). The protein concentration of lysates was

determined using the Pierce™ BCA Protein Assay Kit (Thermo Fisher Scientific) and 30 μg of each sample were separated by SDS-PAGE and transferred to PVDF membrane (Bio-Rad, Hercules, CA). Membranes were blocked with 5% non-fat milk followed by immunoblotting with the primary antibody against rabbit anti-GLUL polyclonal antibody (1:2,000, Bethyl) overnight at 4°C following by rabbit (Cell signaling tech,1:2,000) horseradish peroxidase (HRP)-conjugated secondary antibody (Santa Cruz Biotechnology, 1:2,000). Immune complexes were visualized by means of the ECL Plus detection reagent (Thermo Scientific) and data processed and quantified by the ImageJ software. Protein densities were divided by β-actin densities (mouse monoclonal anti-β-actin, 1:4,000) and the resulting ratio considered as an index of GLUL expression in arbitrary units.

Transduction of HUVECs with shRNA lentiviral particles

shRNA lentiviral particles, including a non-target control (CSHCTR001-1-LVRH1GP) and several shRNA targeting *GLUL* (CS-HSH065270-31-LVRH1GP-01, CS-HSH065270-32-LVRH1GP-01, CS-HSH065270-33-LVRH1GP-01, CS-HSH065270-34-LVRH1GP-01) were purchased from GeneCopoeia. The non-target control contained a scrambled sequence (5'-GCTTCGCGCCGTAGTCTTA-3') not targeting any known human gene, while lentiviruses targeting the *GLUL* gene contain the following sequences: 5'-GCAAGTTCCCACTTAAATAAA-3', 5'-GGCTCTAGTACTTTACAGTCT-3', 5'-CCTGTAAACGGATAATGGACA-3', and 5'-GCACGTGTCTTCTCAATGAAA-3'.

Transductions were performed according to the manufacturer's protocol. Briefly, 0.3×10^6 HUVECs were seeded into a 6-well plate and incubated for 2 days at 37°C in a 5% CO_2 incubator. Cells were infected overnight with control (scramble) and *GLUL* lentiviral particles at multiplicities of infection (MOI) of 1, 3, 5 and 10 in the presence of 8 μg/ml Polybrene transfection reagent (Millipore). Negative control wells included cells not infected with virus and with the addition of Polybrene. All cells were incubated in fresh complete medium for 2 more days for a total of 72 hours since the beginning of transduction. Reduction of GLUL protein expression was confirmed by Western blotting (see above).

For some experiments, following transduction with *GLUL* shRNA, cells were supplemented with glutamine (Sigma-Aldrich) at a final concentration of 10 mmol/L when the medium was changed.

Evaluation of oxidized tyrosines

Cells were plated in 100 mm petri dishes at a concentration of 1.5 x 10^6. When 70% confluence was reached, cells were cultured in basal conditions (5.5 mM D-glucose) or treated with high glucose (25 mM D-glucose) for 48 hours. Cells were washed twice with PBS and then 1 ml of PBS supplemented with 0.005% butylatedhydroxytoluene (BHT) was added to each plate. Cells were scraped, collected in cryotubes and immediately stored at -80°C. As markers of oxidative stress, protein-bound oxidized tyrosine moieties, 3-nitrotyrosine, 3-chlorotyrosine and o,o'-dityrosine were quantified in in cell extracts using isotope dilution high-performance liquid chromatography electrospray ionization tandem MS (HPLC-ESI-MS/MS) as described previously (10). Briefly, the cell lysates were subjected to protein precipitation with ice-cold trichloroacetic acid (10% vol/vol), delipidated with water/methanol/water-washed diethyl ether (1:3:7 vol/vol/vol) and known amounts of isotopically labeled internal standards $^{13}C_6$-tyrosine and $^{13}C_6$—3-nitrotyrosine, $^{13}C_6$—3-chlorotyrosine, and $^{13}C_{12}$--o,o'-dityrosine were added. These preparations were further hydrolyzed at 110°C for 24 hours in 4 M methanesulfonic acid solution saturated with 1% benzoic acid and subject to solid-phase extraction. The oxidized amino acids were quantified by HPLC-ESI-MS/MS with multiple reactions monitoring by integrating peak areas of the labeled standards and the analytes. The levels of the oxidized amino acids were then normalized to the precursor amino acid tyrosine content. The levels of oxidized tyrosine products are expressed as the ratio of the oxidized product over the total tyrosine.

Measurement of methylglyoxal levels

Methylglyoxal protein adducts in 62 HUVEC protein lysates and in the cultures where *GLUL* was downregulated were quantified by the OxiSelect™ Methylglyoxal enzyme immunoassay (Cat. No STA-811, Cell Biolabs, Inc., San Diego, CA) according to the manufacturer's protocol. Briefly, after determining protein concentrations with the Pierce™ BCA Protein Assay Kit (Thermo Fisher Scientific) samples were diluted with 1X PBS to a volume sufficient to load 50 μg of total protein per well. Methylglyoxal-BSA standards or protein samples were absorbed onto a 96-well plate overnight at 4 °C, and then exposed to an anti-methylglyoxal specific monoclonal antibody for 1 hour at room temperature, followed by exposure to a horseradish peroxidase (HRP)-conjugated secondary antibody. The methylglyoxal protein adduct content in experimental samples was determined by comparing its absorbance with that of a methylglyoxal-Bovine Serum Albumin standard curve.

Statistical analysis

The measured values of metabolites obtained from Metabolon were normalized in terms of raw area counts, and these values were then rescaled to set the median equal to 1. Metabolites below the detection limit (Supplementary Table 1) were imputed with the minimum value. Values for each metabolite were then normalized by the median values from each HUVEC sample. Each median-scaled metabolite was then $\log_2$ transformed to approximate the normal distribution. In the present analysis, 35 metabolites involved in glutamic acid metabolism, the γ-glutamyl cycle, and glutathione metabolism were extracted from a larger Metabolon panel of 597 metabolites, as described above under Metabolite Measurements. The association between each metabolite (dependent variable) and rs10911021 (independent variable) was analyzed separately in the low and high glucose experiments by linear mixed effects models, with the SNP considered as a fixed effect according to an additive model (i.e., as number of copies of the risk allele C), and the Metabolon analytical block as random effects. Linear mixed effects models were similarly used for the combined analysis of low and high glucose experiments, including glucose and rs10911021 as fixed effects and HUVEC ID and Metabolon analytical block as random

effects. The modifying effects of glucose on the SNP's association with the metabolites were assessed by incorporating SNP x glucose interaction terms in the main effects mixed models. A similar approach (linear regression or mixed linear models, as appropriate) was applied to the analysis of other variables measured outside of the Metabolon platform such as GLUL protein levels, and methylglyoxal and oxidized tyrosine cell contents. Analyses were normalized by "assay batch" if data were generated in different experiments. All analyses were conducted in SAS v.9.4 (SAS Institute Inc., Cary, NC). Volcano plots were generated in R (R Core Team, Vienna, Austria). Since the study examined a pre-specified hypothesis and most of the metabolites were correlated with each other, an unadjusted p value of less than 0.05 was considered as significant.

RESULTS

HUVEC strain characteristics

The association between rs10911021 genotype and intracellular levels of metabolites involved in glutamic acid metabolism and the gamma-glutamyl cycle was evaluated in primary HUVEC strains isolated from 62 newborns. Thirty of these HUVECs were homozygous for the rs10911021 C allele (C/C), 21 were heterozygous (C/T), and 11 were homozygous for the T allele (T/T). Cells were grown in low (5.5 mM) and high (25 mM) glucose. Consistent with the previously reported association between rs10911021 and GLUL expression levels in HUVECs, cells carrying the C/C genotype had 36% lower GLUL protein levels than those with the T/T genotype when grown in low glucose, with heterozygous cells having intermediate levels (p=0.03, Fig. 1). A similar trend was observed in cells grown in high glucose although the difference among genotypes was smaller and did not reach statistical significance (Fig. 1).

Effect of rs10911021 genotype on metabolites related to glutamic acid metabolism and γ-glutamyl cycle

A total of 35 metabolites were included in this targeted metabolomic analysis, including 14 related to glutamic acid metabolism and 21 related to the γ-glutamyl cycle and glutathione metabolism

(Supplementary Table 1 and Table 2). As shown by the volcano plots in Fig. 2, five metabolites (γ-glutamyl threonine, γ-glutamyl-leucine, γ-glutamyl-isoleucine, γ-glutamyl-valine, and β-citryl-glutamate) showed a significant association ($p<0.05$) with the genotype in both low and high glucose, two (ophthalmate and N-acetyl-aspartyl-glutamate) only in low glucose, and another two (S-lactoyl-glutathione and γ-glutamyl-cysteine) only in high glucose (Fig. 2 and Supplementary Table 2). In a joint analysis of low and high glucose experiments, all the above metabolites were significantly associated with the rs10911021 genotype, with no evidence of genotype x glucose interaction (Fig. 2 and Supplementary Table 2). All nine metabolites showed a significant correlation with one or more of the other metabolites in the group (Supplementary Table 3). Eight of the metabolites (the five γ-glutamyl amino acids, beta-citryl-glutamate, ophthalmate, and N-acetyl-aspartyl-glutamate) were positively associated with the C allele, *i.e.*, their levels rose with the increasing dosage of this allele (Fig. 3). The strongest effect was observed for γ-glutamyl-threonine (+58% per copy of the C allele), followed by ophthalmate (+36%), and γ-glutamyl-valine (+35%) (Fig. 3 and Supplementary Table 2). One of the nine metabolites (S-lactoyl-glutathione) showed instead a negative association with rs10911021. This was especially evident in high glucose conditions, in which cells carrying the C allele had 80% lower levels of S-lactoyl-glutathione than T/T cells (Fig. 3 and Supplementary Table 2). These associations were not affected by adjustment for GLUL protein levels.

No association was detected between rs10911021 and intracellular levels of glutamate or glutamine (the substrate and the product, respectively, of the enzymatic reaction catalyzed by GLUL) or with glutathione (GSH, the product of the γ-glutamyl cycle) in either low or high glucose or in a joint analysis of the two conditions (Supplementary Table 2 and Supplementary Fig. 1). However, in both low and high glucose conditions, the ratio between GSH and glutamate levels was inversely correlated with the dosage of the C allele (Fig. 4A), with an average 9% decrease per allele copy. Also, in both conditions, the GSH/glutamate ratio showed a highly significant inverse correlation with γ-glutamyl-

isoleucine, γ-glutamyl-leucine, γ-glutamyl-valine , γ-glutamyl-threonine, and ophthalmate (Fig. 4B and Supplementary Table 4).

Effect of rs10911021 genotype on methylglyoxal levels

S-lactoyl-glutathione – the only metabolite showing a negative association with rs10911021 allele C – originates in part from the glutathione-mediated detoxification of the reactive compound methylglyoxal - a glycolysis side product. Methylglyoxal is a precursor of advanced glycation end products (AGEs), which have been implicated in the etiology of the vascular complications of diabetes (11). Since S-lactoyl-glutathione levels were lower in allele C carrying cells (Fig. 3), we hypothesized that the C allele was associated with defective methylglyoxal detoxification. Indeed, each additional copy of the C allele was associated with a 69% (p=0.003) and 45% (p=0.03) increase in methylglyoxal levels in cultures exposed to low and high glucose, respectively (Fig. 5A). As compared to HUVECs with the T/T genotype, cells homozygous for the C allele had 2.8-fold higher methylglyoxal levels in low glucose and 2.1-fold higher levels in high glucose, with heterozygous cells having intermediate levels in both conditions (Fig. 5A). The rs10911021 genotype had little or no effect on other intracellular markers of oxidative stress such as oxidized tyrosines. The only significant association was with 3-chloro-tyrosine levels in 25 mM glucose, but the effect of the genotypes with this metabolite was much smaller than that on methylglyoxal levels (Supplementary Fig. 2).

To assess whether the lower GLUL levels associated with the allele C were responsible for the higher methylglyoxal levels observed in cells carrying this allele, GLUL protein levels were down-regulated by means of shRNA transfection in 14 different HUVEC strains. On average, GLUL protein levels were 43% lower ($p<0.0001$) in cells transfected with a shRNA targeting GLUL than in the same cells transfected with a scrambled shRNA (Fig. 5B). Such reduction in GLUL levels was accompanied by a 40% increase in methylglyoxal levels (p=0.03) (Fig. 5C). This was completely prevented (p=0.0004) by

exposing cells to increased concentrations of glutamine – the product of the enzymatic reaction catalyzed by GLUL (Fig. 5C).

DISCUSSION

In the present study, we used a targeted metabolomic approach to investigate the association between the 1q25 CHD locus and intracellular levels of 35 metabolites involved in glutamic acid metabolism and γ-glutamyl cycle in 62 HUVEC strains naturally carrying different genotypes for the 1q25 lead variant rs10911021. This analysis was based on the hypothesis of an impairment of the γ-glutamyl cycle and/or glutamic acid metabolism as the mechanism linking the 1q25 locus to CHD, which was prompted by our previous finding of an association of the 1q25 risk allele with decreased expression of the nearby *GLUL* (glutamate-ammonia ligase) gene in endothelial cells and with lower pyroglutamic-to-glutamic acid ratio in plasma (3). Our data, demonstrating differences among 1q25 genotypes in the cellular content of nine metabolites related to the γ-glutamyl cycle and glutamic acid metabolism, and the AGE precursor methylglyoxal, which is normally detoxified by GSH, support this hypothesis.

Of the nine metabolites displaying a significant association with the 1q25 variant, eight, including five γ-glutamyl amino acids, ophthalmate, beta-citryl-glutamate, and N-acetyl-aspartyl-glutamate, had increased levels in HUVECs carrying the 1q25 risk allele. Since all these metabolites include a glutamyl residue, their increased levels may indicate an imbalance between the increased availability of glutamic acid (resulting from the decreased activity of GLUL associated with the risk allele), and the availability of cysteine for the synthesis of γ-glutamyl cysteine by glutamate cysteine ligase (GCL, the γ-glutamyl cycle rate limiting enzyme). Under these conditions, the excess glutamic acid may be transferred to other amino acids by GCL leading to increased synthesis of γ-glutamyl amino acids other than γ-glutamyl cysteine (12) (Fig. 6). A similar mechanism can be hypothesized for the increased

levels of ophthalmate - a tri-peptide analog of GSH without its anti-oxidant properties - resulting from the GCL-mediated transfer of glutamic acid to L-2-aminobutyrate (rather than cysteine) followed by the addition of glycine (13) (Fig. 6). The increase in ophthalmate and other glutamyl-containing molecules, which is similar to that observed in situations of increased oxidative stress (14), suggests an inefficient utilization of glutamic acid towards the synthesis of GSH in endothelial cells carrying the 1q25 risk allele. Indeed, while GSH levels were not significantly different among 1q25 genotypes, the ratio between GSH and glutamate levels was inversely correlated to the risk allele dosage in both low and high glucose. Also, in both conditions, the GSH/glutamate ratio showed a highly significant inverse correlation with γ-glutamyl-isoleucine, γ-glutamyl-leucine, γ-glutamyl-valine , γ-glutamyl-threonine, and ophthalmate.

Given that the CHD-predisposing effect of the 1q25 locus found in previous studies was specific to persons with diabetes (3), the finding of a similar association between genotype and intracellular metabolic features in low and high glucose, i.e., the lack of SNP x glucose interaction, deserves a comment. A possible explanation is that glucose exposure for 48 hours did not adequately reproduce the effects of chronic exposure to high glucose occurring in people with diabetes. Alternatively, the interaction between 1q25 and diabetic milieu on CHD risk observed *in vivo* may be mediated by other metabolic characteristics typical of type 2 diabetes, such as insulin-resistance and/or dyslipidemia (15), rather than hyperglycemia itself. The possible interaction of the 1q25 genotype with these additional diabetes-associated exposures will have to be investigated in further studies.

Alone among the metabolites associated with the 1q25 locus, S-lactoyl-glutathione showed a negative association with the 1q25 genotypes, its level being markedly reduced in cells homozygous for the risk allele. S-lactoyl-glutathione is mostly generated from glutathione in the glyoxalase system during the detoxification of methylglyoxal, which is a highly toxic by-product of glucose and lipid metabolism that has been implicated in the etiology of vascular complications of diabetes as a precursor of AGEs (11; 16-19). Methylglyoxal reacts with GSH to form a thiohemiacetal (16), which is

converted into S-lactoyl-glutathione by the enzyme glyoxylase 1 (GLO1) and then to lactate and glutathione by glyoxylase 2 (GLO2) (Fig. 6). Reduced S-lactoyl-glutathione has been associated with dysregulation of hepatic methylglyoxal detoxification in a mouse model of homocystinuria (14). Consistent with a dysregulation of methylglyoxal detoxification, we observed a striking increase in methylglyoxal (2.8-fold in low glucose and 2.1-fold in high glucose) in HUVECs homozygous for the risk allele as compared to cells homozygous for the protective allele. Of note, GLUL down-regulation through shRNA interference significantly increased methylglyoxal levels, supporting the hypothesis that the association between 1q25 risk allele and methylglyoxal levels is sustained by a cause-effect relationship. The mechanism underlying this effect may relate to the inefficient synthesis of GSH described above, despite the apparent lack of significant differences in absolute GSH levels among 1q25 genotypes. This hypothesis is supported by our finding of another marker of oxidative stress (3-chloro-tyrosine) (20) being significantly associated with the risk allele in HUVECs exposed to high glucose as well as by a report in the literature describing an association of the 1q25 risk allele with lower plasma levels of GSH and higher levels of the oxidative stress biomarker malondialdeheyde (21). Another possibility to explain the mechanism triggering the observed association is inhibition of GLO1 activity by some of the metabolites such as γ-glutamyl-amino acids or ophthalmate that are increased in risk allele carriers and have been shown to impact cellular transporters and signaling (13; 22).

Important for translating our findings to develop new interventions to prevent CHD in diabetes, the increase in methylglyoxal levels associated with GLUL down-regulation was prevented by increasing the culture medium concentration of glutamine five times above the levels normally used to preserve cell functions during prolonged periods of incubation (9). Glutamine is a known precursor of nicotinamide adenine dinucleotide (NAD) and oral supplementation of this amino acid has been shown to raise the NAD redox ratio in red blood cells from patients with sickle cell anemia (23) and to be associated with clinical improvement in the frequency of sickle cell crises in a phase 3 clinical trial (24).

If the beneficial effect on methylglyoxal production by vascular cells is confirmed by further studies and is also demonstrated in animal models of atherosclerosis, glutamine supplementation may be considered as a candidate intervention for CHD prevention among individuals with type 2 diabetes who carry the 1q25 risk allele and have lower glutamine synthase activity.

Our study has several strengths including the use of a large number of untransformed human primary cells, through which cellular functions could be studied without artifacts deriving from immortalization, the availability of cells from multiple subjects, allowing the study of naturally occurring genetic variants, without the need for genetic manipulation, and the systematic assessment of a large panel of metabolites involved in glutamic acid metabolism and the γ-glutamyl cycle. However, some potential limitations must be acknowledged. While HUVECs have been extensively used for *in vitro* studies of the impact of diabetes on the endothelium (25; 26), their metabolic characteristics and response to stimuli may not perfectly capture those of endothelial cells lining the coronary arteries (27). Also, while our study provided an innovative snapshot of the metabolic differences between 1q25 genotypes based on the cell content of key metabolites, inferences made on the basis of these data will have to be corroborated by more detailed studies of metabolic fluxes and enzymatic activities. Finally, our study was focused on the metabolic traits associated with the 1q25 risk allele. However, we cannot exclude that non-metabolic effects also contribute to the increased CHD risk associated with this locus as suggested by the recent report of an unexpected role of glutamate-ammonia ligase (the enzyme coded by *GLUL*) in angiogenesis (28). Also, we cannot exclude a role of changes in the expression of other genes, although *GLUL* was the only one of the eight genes in the 1q25 region analyzed in the original report for which a significant association was observed between mRNA levels and rs10911021 (3). Finally, no adjustment for multiple comparisons was made. While this was based on the pre-specified nature of the analysis and on the high correlation among the metabolites included in this study, the possibility of false positives results cannot be excluded.

In summary, our findings in a unique collection of HUVEC strains from multiple individuals provide further support for an association between the diabetes-specific CHD locus at 1q25 and alterations of glutamic acid metabolism and the γ-glutamyl cycle. They also suggest decreased GSH-mediated detoxification of the AGE-precursor methylglyoxal as a mechanism linking this locus to increased CHD risk and raise the hypothesis of glutamine supplementation as an approach to prevent CHD in carriers of this genetic risk factor.

Acknowledgments

We thank Dr Pamela Di Tomo for her skilled technical assistance in HUVECs harvesting and banking.

Data and Resource Availability. The datasets generated during and/or analyzed during the current study are available from the corresponding author upon request.

Author Contributions

CP and AD designed the study, acquired, analyzed, and interpreted the data, wrote the initial draft of the manuscript and revised the manuscript to its final form. HS analyzed and interpreted the data, and revised the manuscript to its final form. SaP, AP, and VT contributed to the study design, interpreted the data, and revised the manuscript to its final form. NDP, KP, LZ, and SuP acquired, analyzed and interpreted data, and revised the manuscript to its final form. The content of the paper is solely the responsibility of the authors and does not necessarily represent the official views of the National Institutes of Health or other funding entities. AD is the guarantors of this work and, as such, had full access to all the data in the study and take responsibility for the integrity of the data and the accuracy of the data analysis.

Funding

This research was supported by a research grant from Sanofi-Aventis (to A.D.), NIH grant DK36836 (Molecular Phenotyping and Genotyping Core and Enrichment Core of the Diabetes Research Center at the Joslin Diabetes Center), NIH grants DK081943 and DK082841 (to Su.P.), the Italian Ministry of Health (Ricerca Corrente 2019-2020 to V.T and 2018-2020 to Sa.P.), the Italian Ministry of University and Research (PRIN 2015 to V.T.), and Fondazione Roma (Grant for Biomedical Research: Non Communicable Diseases, Call for proposals 2013 to V.T.).

Duality of Interest

CP, HS, SaP, NDP, LZ, KP, VT, SuP, and AP have nothing to disclose. AD reports a grant from Sanofi Aventis supporting the submitted work.

Prior Presentation

This study was presented as a poster at the 79th Scientific Sessions of the American Diabetes Association, San Francisco, California, 7–11 June 2019.

REFERENCES

1. Fox CS, Coady S, Sorlie PD, D'Agostino RB, Sr., Pencina MJ, Vasan RS, Meigs JB, Levy D, Savage PJ: Increasing cardiovascular disease burden due to diabetes mellitus: the Framingham Heart Study. Circulation 2007;115:1544-1550
2. Doria A: Leveraging Genetics to Improve Cardiovascular Health in Diabetes: The 2018 Edwin Bierman Award Lecture. Diabetes 2019;68:479-489
3. Qi L, Qi Q, Prudente S, Mendonca C, Andreozzi F, di PN, Sturma M, Novelli V, Mannino GC, Formoso G, Gervino EV, Hauser TH, Muehlschlegel JD, Niewczas MA, Krolewski AS, Biolo G, Pandolfi A, Rimm E, Sesti G, Trischitta V, Hu F, Doria A: Association between a genetic variant related to glutamic acid metabolism and coronary heart disease in individuals with type 2 diabetes. JAMA 2013;310:821-828
4. Look Ahead Research Group: Prospective Association of GLUL rs10911021 With Cardiovascular Morbidity and Mortality Among Individuals With Type 2 Diabetes: The Look AHEAD Study. Diabetes 2016;65:297-302
5. Prudente S, Shah H, Bailetti D, Pezzolesi M, Buranasupkajorn P, Mercuri L, Mendonca C, De CS, Niewczas M, Trischitta V, Doria A: Genetic variant at the GLUL locus predicts all-cause mortality in patients with type 2 diabetes. Diabetes 2015;64:2658-2663
6. Krebs HA: Metabolism of amino-acids: The synthesis of glutamine from glutamic acid and ammonia, and the enzymic hydrolysis of glutamine in animal tissues. Biochem J 1935;29:1951-1969
7. Reid M, Jahoor F: Glutathione in disease. Curr Opin Clin Nutr Metab Care 2001;4:65-71
8. Forstermann U, Xia N, Li H: Roles of Vascular Oxidative Stress and Nitric Oxide in the Pathogenesis of Atherosclerosis. Circ Res 2017;120:713-735
9. Di Tomo P, Lanuti P, Di Pietro N, Baldassarre MPA, Marchisio M, Pandolfi A, Consoli A, Formoso G: Liraglutide mitigates TNF-alpha induced pro-atherogenic changes and microvesicle release in HUVEC from diabetic women. Diabetes Metab Res Rev 2017;33
10. Vivekanandan-Giri A, Byun J, Pennathur S: Quantitative analysis of amino Acid oxidation markers by tandem mass spectrometry. Methods Enzymol 2011;491:73-89
11. Thornalley PJ: Glyoxalase I--structure, function and a critical role in the enzymatic defence against glycation. Biochem Soc Trans 2003;31:1343-1348
12. Bachhawat AK, Yadav S: The glutathione cycle: Glutathione metabolism beyond the gamma-glutamyl cycle. IUBMB Life 2018;70:585-592
13. Dello SA, Neis EP, de Jong MC, van Eijk HM, Kicken CH, Olde Damink SW, Dejong CH: Systematic review of ophthalmate as a novel biomarker of hepatic glutathione depletion. Clin Nutr 2013;32:325-330
14. Maclean KN, Jiang H, Aivazidis S, Kim E, Shearn CT, Harris PS, Petersen DR, Allen RH, Stabler SP, Roede JR: Taurine treatment prevents derangement of the hepatic gamma-glutamyl cycle and methylglyoxal metabolism in a mouse model of classical homocystinuria: regulatory crosstalk between thiol and sulfinic acid metabolism. FASEB J 2018;32:1265-1280
15. Warram JH, Kopczynski J, Janka HU, Krolewski AS: Epidemiology of non-insulin-dependent diabetes mellitus and its macrovascular complications. A basis for the development of cost-effective programs. Endocrinol Metab Clin North Am 1997;26:165-188
16. Maessen DE, Stehouwer CD, Schalkwijk CG: The role of methylglyoxal and the glyoxalase system in diabetes and other age-related diseases. Clin Sci (Lond) 2015;128:839-861
17. Schalkwijk CG, Stehouwer CDA: Methylglyoxal, a Highly Reactive Dicarbonyl Compound, in Diabetes, Its Vascular Complications, and Other Age-Related Diseases. Physiol Rev 2020;100:407-461
18. Hanssen NMJ, Scheijen J, Jorsal A, Parving HH, Tarnow L, Rossing P, Stehouwer CDA, Schalkwijk CG: Higher Plasma Methylglyoxal Levels Are Associated With Incident Cardiovascular Disease in Individuals With Type 1 Diabetes: A 12-Year Follow-up Study. Diabetes 2017;66:2278-2283

19. van Eupen MG, Schram MT, Colhoun HM, Hanssen NM, Niessen HW, Tarnow L, Parving HH, Rossing P, Stehouwer CD, Schalkwijk CG: The methylglyoxal-derived AGE tetrahydropyrimidine is increased in plasma of individuals with type 1 diabetes mellitus and in atherosclerotic lesions and is associated with sVCAM-1. Diabetologia 2013;56:1845-1855
20. Shao B, Pennathur S, Heinecke JW: Myeloperoxidase targets apolipoprotein A-I, the major high density lipoprotein protein, for site-specific oxidation in human atherosclerotic lesions. J Biol Chem 2012;287:6375-6386
21. Shahid SU, Shabana, Humphries S: The SNP rs10911021 is associated with oxidative stress in coronary heart disease patients from Pakistan. Lipids Health Dis 2018;17:6
22. Broadhead GK, Mun HC, Avlani VA, Jourdon O, Church WB, Christopoulos A, Delbridge L, Conigrave AD: Allosteric modulation of the calcium-sensing receptor by gamma-glutamyl peptides: inhibition of PTH secretion, suppression of intracellular cAMP levels, and a common mechanism of action with L-amino acids. J Biol Chem 2011;286:8786-8797
23. Niihara Y, Zerez CR, Akiyama DS, Tanaka KR: Oral L-glutamine therapy for sickle cell anemia: I. Subjective clinical improvement and favorable change in red cell NAD redox potential. Am J Hematol 1998;58:117-121
24. Niihara Y, Miller ST, Kanter J, Lanzkron S, Smith WR, Hsu LL, Gordeuk VR, Viswanathan K, Sarnaik S, Osunkwo I, Guillaume E, Sadanandan S, Sieger L, Lasky JL, Panosyan EH, Blake OA, New TN, Bellevue R, Tran LT, Razon RL, Stark CW, Neumayr LD, Vichinsky EP, Investigators of the Phase 3 Trial of l-Glutamine in Sickle Cell D: A Phase 3 Trial of l-Glutamine in Sickle Cell Disease. N Engl J Med 2018;379:226-235
25. Lorenzi M, Cagliero E, Toledo S: Glucose toxicity for human endothelial cells in culture. Delayed replication, disturbed cell cycle, and accelerated death. Diabetes 1985;34:621-627
26. Castellano I, Di Tomo P, Di Pietro N, Mandatori D, Pipino C, Formoso G, Napolitano A, Palumbo A, Pandolfi A: Anti-Inflammatory Activity of Marine Ovothiol A in an In Vitro Model of Endothelial Dysfunction Induced by Hyperglycemia. Oxid Med Cell Longev 2018;2018:2087373
27. Garcia-Cardena G, Comander J, Anderson KR, Blackman BR, Gimbrone MA, Jr.: Biomechanical activation of vascular endothelium as a determinant of its functional phenotype. Proc Natl Acad Sci U S A 2001;98:4478-4485
28. Eelen G, Dubois C, Cantelmo AR, Goveia J, Bruning U, DeRan M, Jarugumilli G, van Rijssel J, Saladino G, Comitani F, Zecchin A, Rocha S, Chen R, Huang H, Vandekeere S, Kalucka J, Lange C, Morales-Rodriguez F, Cruys B, Treps L, Ramer L, Vinckier S, Brepoels K, Wyns S, Souffreau J, Schoonjans L, Lamers WH, Wu Y, Haustraete J, Hofkens J, Liekens S, Cubbon R, Ghesquiere B, Dewerchin M, Gervasio FL, Li X, van Buul JD, Wu X, Carmeliet P: Role of glutamine synthetase in angiogenesis beyond glutamine synthesis. Nature 2018;561:63-69

Figure legends

Figure 1. GLUL protein levels in HUVECs carrying different rs10911021 genotypes. Distributions of GLUL levels relative to β-actin, expressed as arbitrary units and normalized by assay batch, are shown for 62 HUVEC exposed to 5 mM and 25 mM glucose. Boxes correspond to the interquartile range, the line within the box to the median, and the cross to the mean. Whiskers correspond to the maximum and minimum values.

Figure 2. Association between 1q25 (rs10911021) genotype and 35 metabolites related to glutamate metabolism and γ-glutamyl cycle in HUVECs. Association results are shown for 62 HUVECs exposed to 5 mM and 25 mM glucose and in a joint analysis of the two glucose conditions. The association with the rs10911021 genotype is expressed as log2 fold-change per allele copy (x-axis) and significance is presented as -log10 p-value (y-axis). The dotted line indicates the 0.05 p values threshold. Significant metabolites of interest are indicated by red ($p<0.01$) and purple ($p<0.05$) circles.

Figure 3. Association between 1q25 genotype and metabolite levels in HUVEC. Distributions according to rs10911021 genotype in 62 HUVEC exposed to 5 mM and 25 mM glucose are shown for γ-glutamyl-threonine, γ-glutamyl-leucine, γ-glutamyl-valine, β-citryl-glutamate, γ-glutamyl-isoleucine, S-lactoyl-glutathione, γ-glutamyl-cysteine, ophthalmate, and N-acetyl-aspartyl-glutamate (NAAG). Boxes correspond to the interquartile range, the line within the box to the median, and the cross to the mean. Whiskers correspond to the maximum and minimum values.

Figure 4. GSH/glutamate ratio in HUVECs. A. Distributions of log2 GSH/glutamate ratios according to the 1q25 (rs10911021) genotype in 62 HUVEC exposed to 5 mM and 25 mM glucose. Boxes correspond to the interquartile range, the line within the box to the median, and the cross to the mean. Whiskers

correspond to the maximum and minimum. **B.** Correlations of log2 GSH/glutamate ratio with log2 γ-glutamyl-isoleucine and with log2 ophthalmate in 62 HUVEC exposed to 5 mM and 25 mM glucose.

Figure 5. Methylglyoxal levels in HUVECs. A. Distributions of Log2 levels of methylglyoxal (arbitrary units after normalization by assay batch) in 62 HUVEC exposed to 5 mM and 25 mM glucose. **B.** Distributions of GLUL protein levels (arbitrary units after normalization by β-actin signal intensity and assay batch) in 14 HUVEC transfected with scramble or GLUL-shRNA. Representative Western blot bands are shown below the plot. **C.** Distributions of methylglyoxal levels (arbitrary units after normalization by assay batch) in 14 HUVEC transfected with scramble or GLUL shRNA, with or without glutamine supplementation. Boxes correspond to the interquartile range, the line within the box to the median, and the cross to the mean. Whiskers correspond to the maximum and minimum values

Figure 6. Schematic representation of the γ-glutamyl cycle and glyoxalase system.

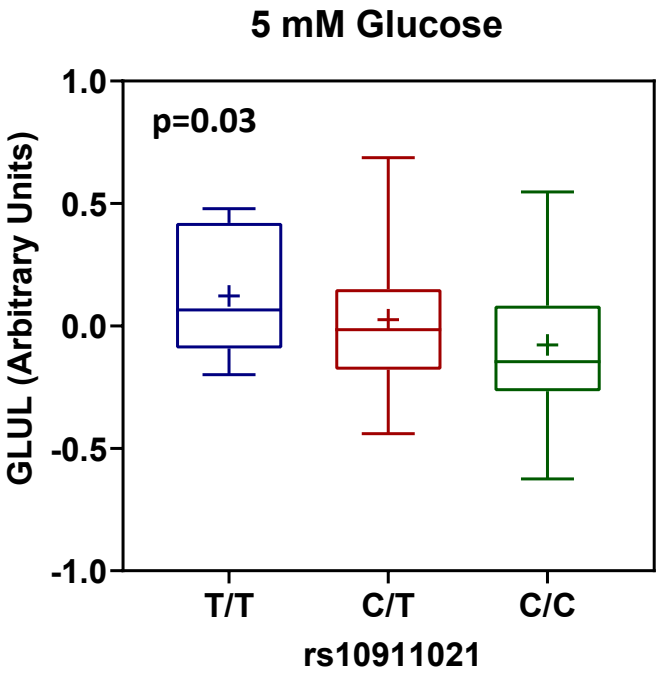
5 mM Glucose
p=0.03
GLUL (Arbitrary Units)
1.0
0.5
0.0
-0.5
-1.0
T/T
C/T
C/C
rs10911021

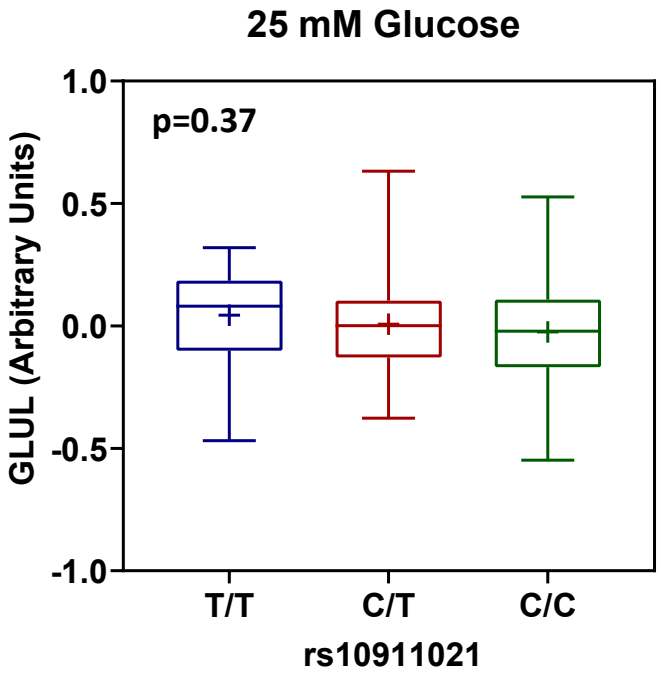
25 mM Glucose
p=0.37
GLUL (Arbitrary Units)
1.0
0.5
0.0
-0.5
-1.0
T/T
C/T
C/C
rs10911021

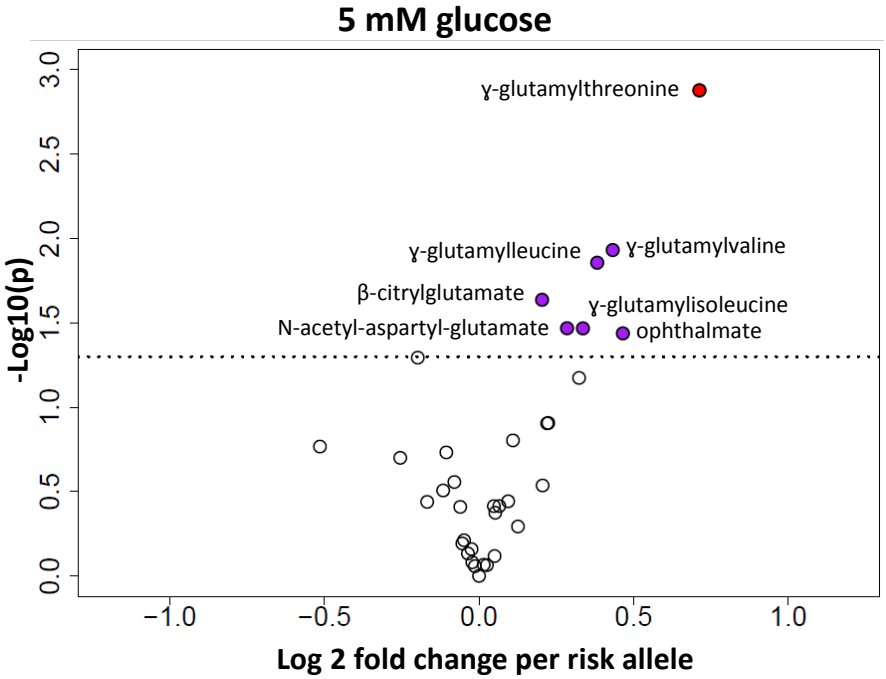
5 mM glucose
ɣ-glutamylthreonine
ɣ-glutamylleucine
ɣ-glutamylvaline
β-citrylglutamate
ɣ-glutamylisoleucine
N-acetyl-aspartyl-glutamate
ophthalmate
-Log10(p)
Log 2 fold change per risk allele

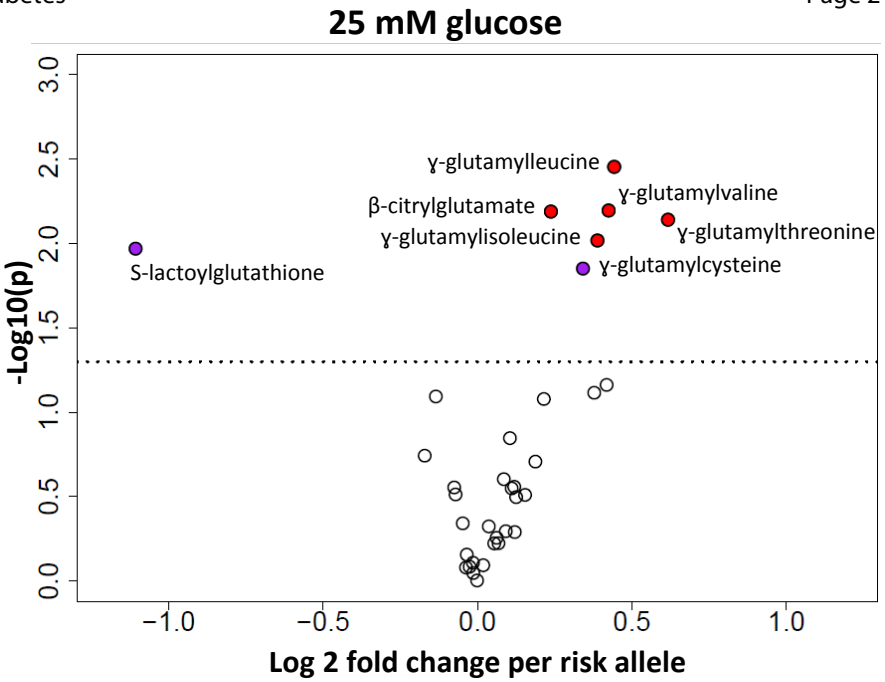
25 mM glucose
ɣ-glutamylleucine
ɣ-glutamylvaline
β-citrylglutamate
ɣ-glutamylisoleucine
ɣ-glutamylthreonine
S-lactoylglutathione
ɣ-glutamylcysteine
-Log10(p)
Log 2 fold change per risk allele

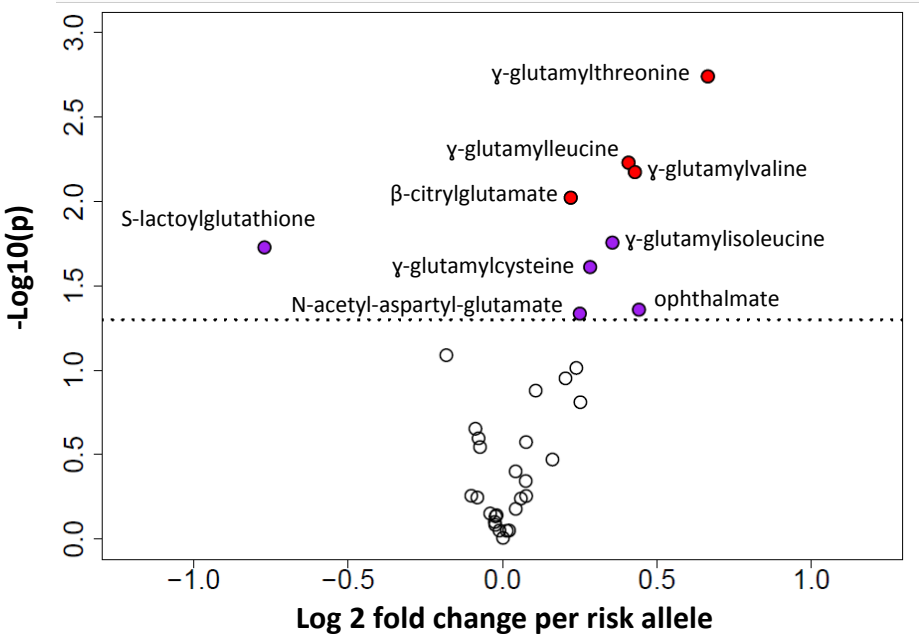
5 mM and 25 mM glucose combined
ɣ-glutamylthreonine
ɣ-glutamylleucine
ɣ-glutamylvaline
β-citrylglutamate
S-lactoylglutathione
ɣ-glutamylisoleucine
ɣ-glutamylcysteine
N-acetyl-aspartyl-glutamate
ophthalmate
-Log10(p)
Log 2 fold change per risk allele

γ-glutamyl-threonine

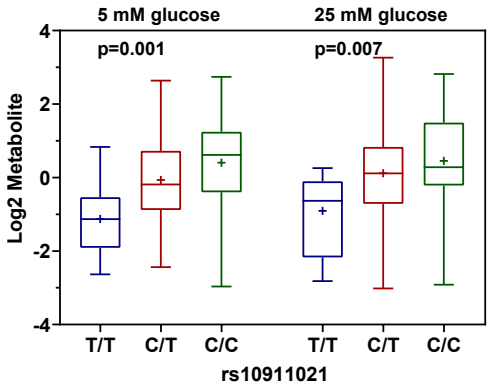

γ-glutamyl-leucine

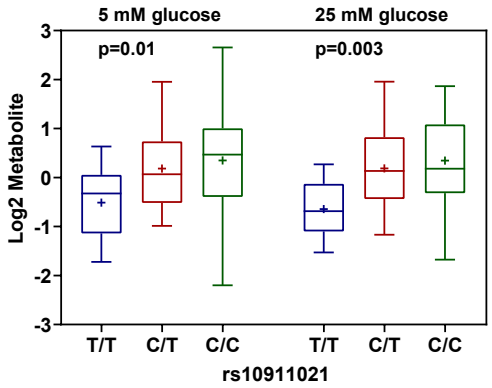

γ-glutamyl-valine

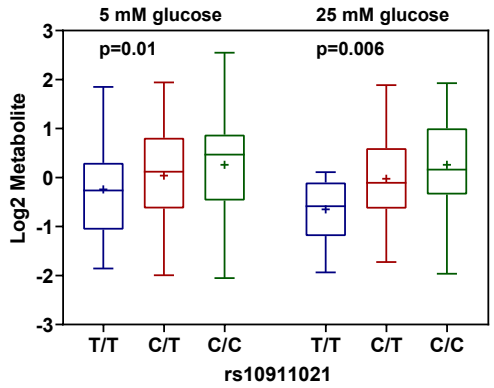

β-citryl-glutamate

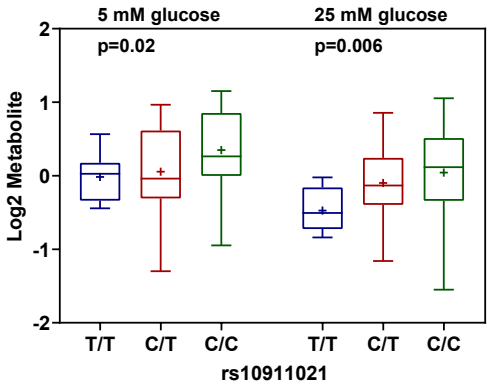

γ-glutamyl-isoleucine

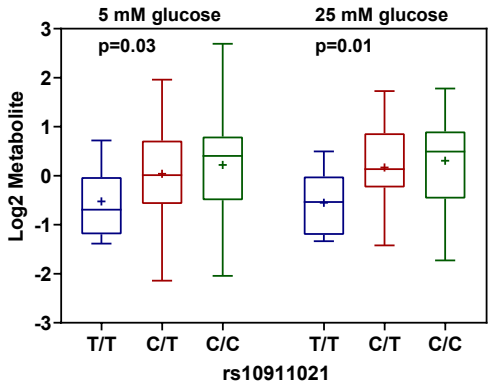

S-lactoyl-glutathione

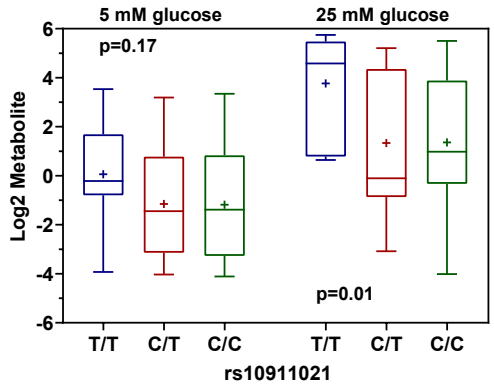

γ-glutamyl-cysteine

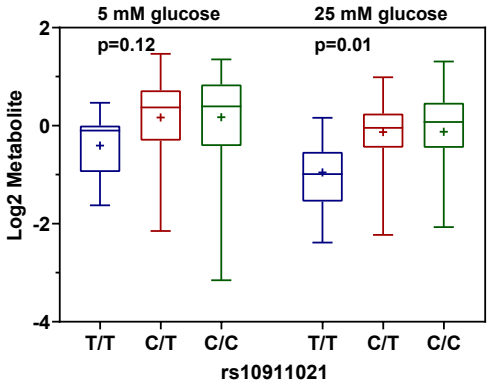

Ophthalmate

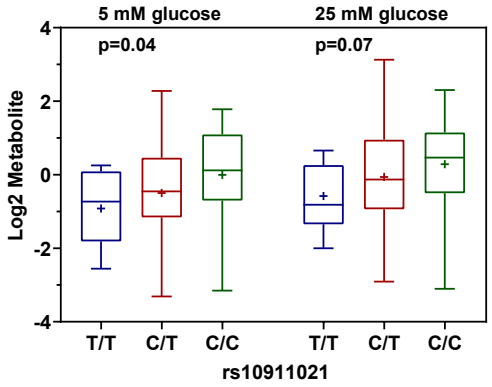

N-acetyl-aspartyl-glutamate (NAAG)

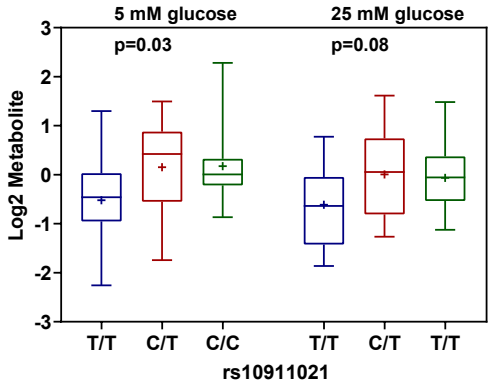

A

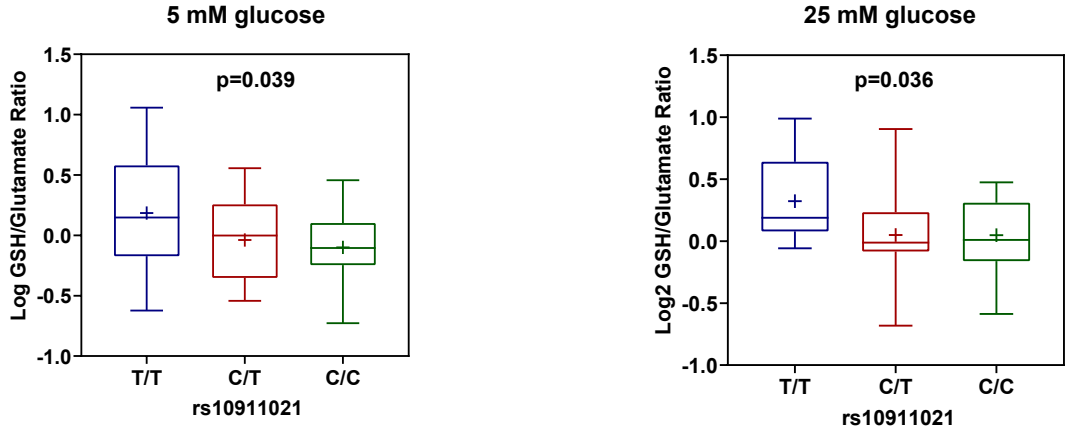
5 mM glucose
p=0.039
Log GSH/Glutamate Ratio
1.5
1.0
0.5
0.0
-0.5
-1.0
T/T
C/T
C/C
rs10911021
25 mM glucose
p=0.036
Log2 GSH/Glutamate Ratio
1.5
1.0
0.5
0.0
-0.5
-1.0
T/T
C/T
C/C
rs10911021

B

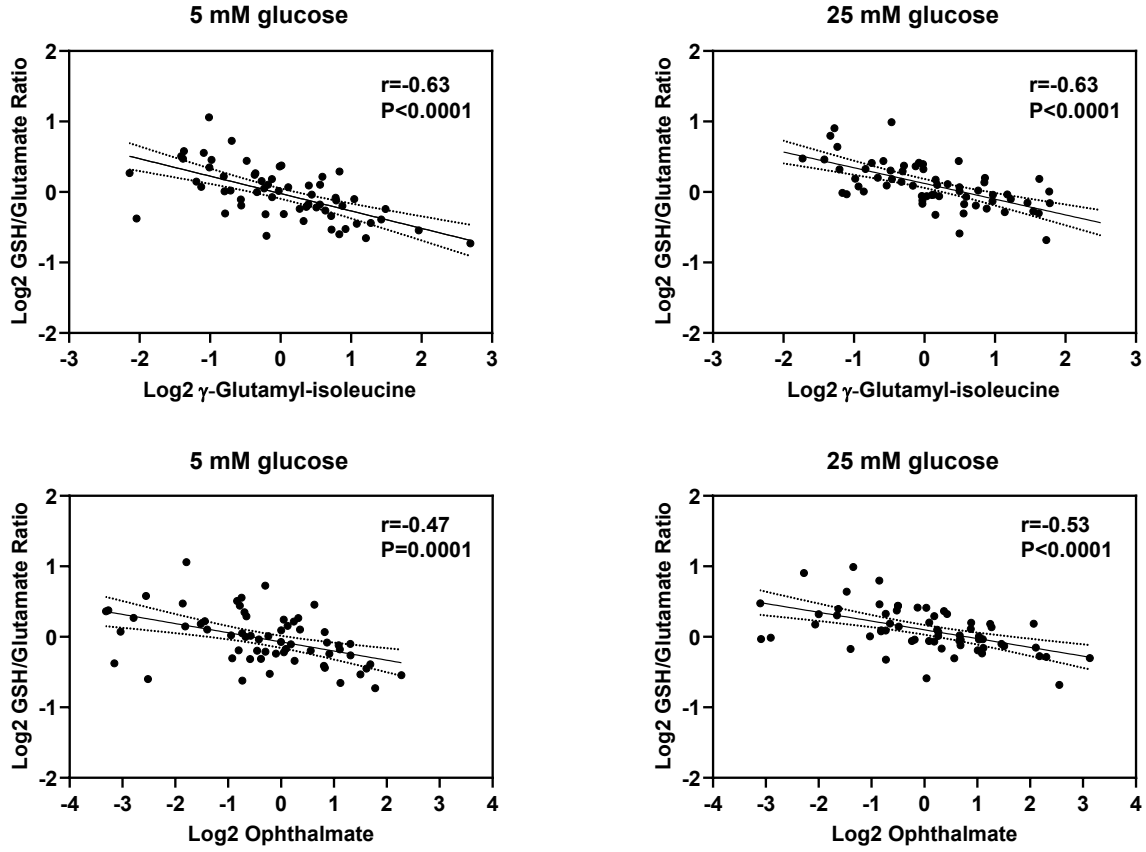
5 mM glucose
r=-0.63
P<0.0001
Log2 GSH/Glutamate Ratio
Log2 γ-Glutamyl-isoleucine
25 mM glucose
r=-0.63
P<0.0001
Log2 GSH/Glutamate Ratio
Log2 γ-Glutamyl-isoleucine
5 mM glucose
r=-0.47
P=0.0001
Log2 GSH/Glutamate Ratio
Log2 Ophthalmate
25 mM glucose
r=-0.53
P<0.0001
Log2 GSH/Glutamate Ratio
Log2 Ophthalmate

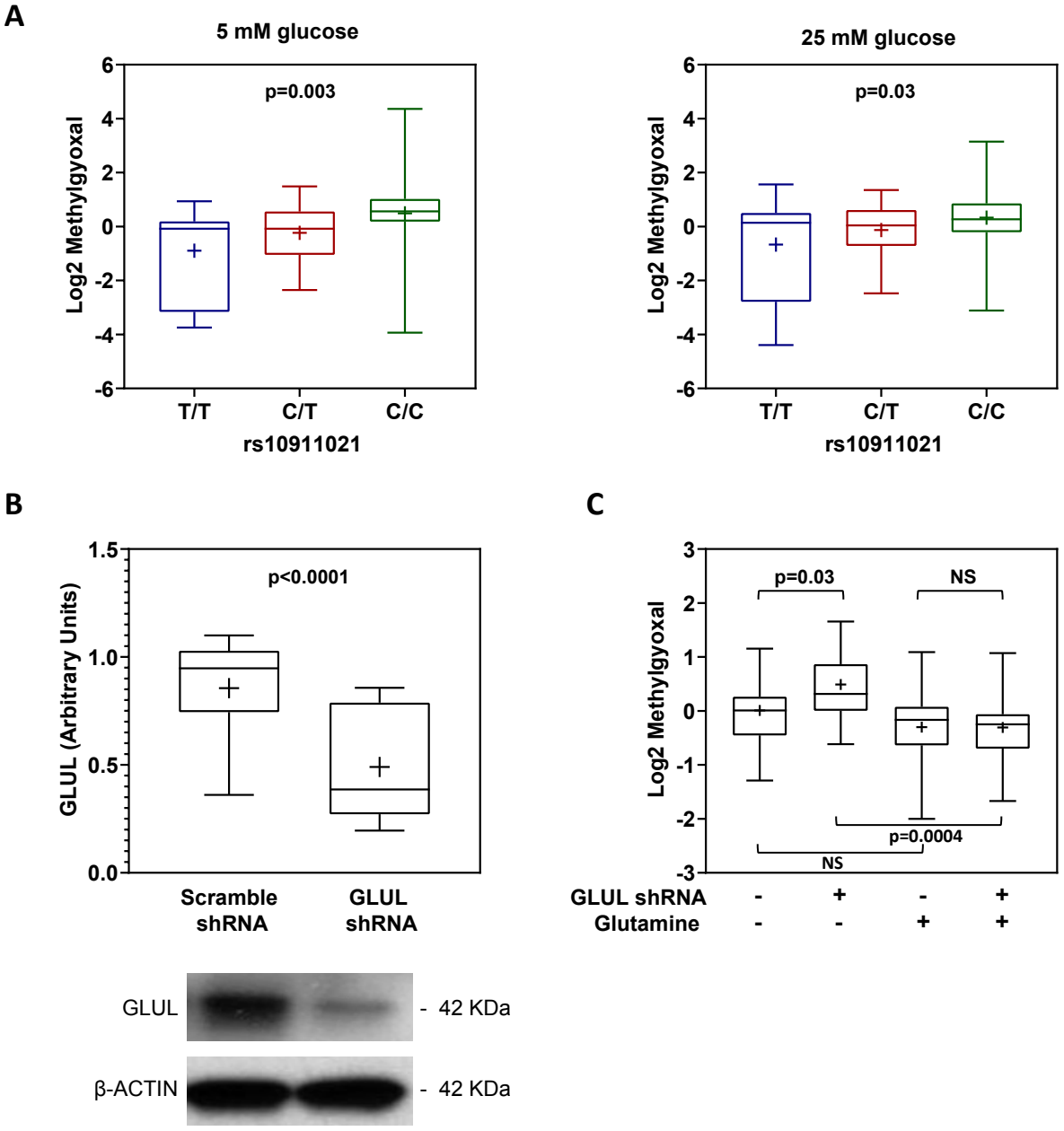
A
5 mM glucose
p=0.003
Log2 Methylgyoxal
6
4
2
0
-2
-4
-6
T/T
C/T
C/C
rs10911021
25 mM glucose
p=0.03
Log2 Methylgyoxal
6
4
2
0
-2
-4
-6
T/T
C/T
C/C
rs10911021
B
p<0.0001
GLUL (Arbitrary Units)
1.5
1.0
0.5
0.0
Scramble shRNA
GLUL shRNA
GLUL
- 42 KDa
β-ACTIN
- 42 KDa
C
p=0.03
NS
p=0.0004
NS
Log2 Methylgyoxal
3
2
1
0
-1
-2
-3
GLUL shRNA - + - +
Glutamine - - + +

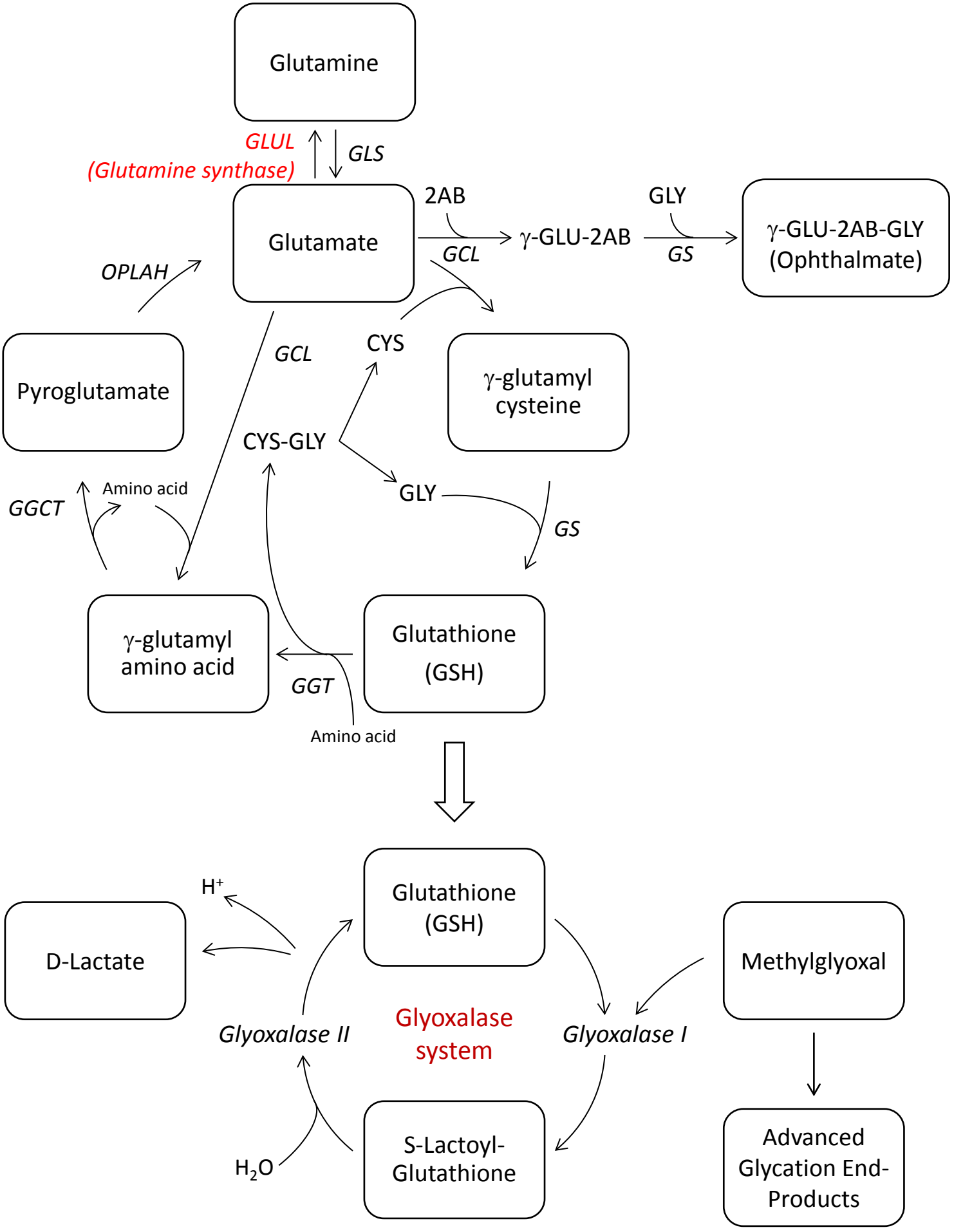
Glutamine
GLUL
(Glutamine synthase)
GLS
Glutamate
2AB
γ-GLU-2AB
GLY
GS
γ-GLU-2AB-GLY
(Ophthalmate)
GCL
OPLAH
Pyroglutamate
GCL
CYS
γ-glutamyl
cysteine
CYS-GLY
GLY
GS
GGCT
Amino acid
γ-glutamyl
amino acid
GGT
Glutathione
(GSH)
Amino acid
Glutathione
(GSH)
H+
D-Lactate
Methylglyoxal
Glyoxalase II
Glyoxalase
system
Glyoxalase I
H2O
S-Lactoyl-
Glutathione
Advanced
Glycation End-
Products

On-Line Only Supplementary Material

Supplement to Pipino, Shah, Prudente, et al. “Association of the 1q25 diabetes-specific coronary heart disease locus with alterations of the γ-glutamyl cycle and increased methylglyoxal levels in endothelial cells.”

Supplementary Table 1. Detection of metabolites in HUVEC extracts.

Metabolite	CHEMICAL_ID	Detection (%)*
gamma-glutamylthreonine	100001314	95.8
gamma-glutamylleucine	1268	100.0
gamma-glutamylvaline	100001126	98.4
beta-citrylglutamate	100003271	100.0
gamma-glutamylisoleucine*	100001485	98.4
S-lactoylglutathione	1343	85.2
gamma-glutamylcysteine	1036	99.2
ophthalmate	100001311	96.7
N-acetyl-aspartyl-glutamate (NAAG)	100001612	99.2
S-nitrosoglutathione (GSNO)	100004662	98.4
glutamate, gamma-methyl ester	100001103	99.2
gamma-glutamylglycine	100001294	25.4
N-acetylglutamate	100000282	100.0
S-1-pyrroline-5-carboxylate	35	76.0
pyroglutamine*	100001540	100.0
glutathione, reduced (GSH)	496	100.0
5-oxoproline	1021	100.0
2-hydroxybutyrate/2-hydroxyisobutyrate	100008928	97.5
4-hydroxy-nonenal-glutathione	100006240	88.3
glutamate	561	100.0
gamma-aminobutyrate (GABA)	141	100.0
gamma-glutamylglutamine	1140	100.0
glutamine	563	100.0
alpha-ketoglutarate	93	100.0
gamma-glutamylphenylalanine	100000491	79.6
gamma-glutamyl-epsilon-lysine	100001262	100.0
4-hydroxyglutamate	100002544	97.5
glycine	340	100.0
gamma-carboxyglutamate	100002679	100.0
cysteinylglycine	278	100.0
cysteine	800	100.0
carboxyethyl-GABA	100003260	30.1
gamma-glutamylglutamate	331	100.0
N-acetylglutamine	100001253	100.0
glutathione, oxidized (GSSG)	448	100.0

*Percent of HUVEC with metabolite levels above detection limit.

Supplementary Table 2. Association between rs10911021 C allele and metabolites related to glutamic acid metabolism and the γ-glutamyl cycle.

Metabolite	SNP effect in low glucose				SNP effect in high glucose				SNP effect in low+high glucose				SNP x glucose interaction
	Est*	95% CI		P	Est*	95% CI		P	Est*	95% CI		P	Inter_p
gamma-glutamylthreonine	64%	23%	118%	**0.001**	53%	14%	107%	**0.007**	58%	20%	109%	**0.002**	0.510
gamma-glutamylleucine	30%	6%	60%	**0.014**	36%	12%	65%	**0.004**	33%	9%	61%	**0.006**	0.522
gamma-glutamylvaline	35%	8%	69%	**0.012**	34%	9%	64%	**0.006**	35%	9%	66%	**0.007**	0.926
beta-citrylglutamate	15%	2%	30%	**0.023**	18%	5%	32%	**0.006**	17%	4%	30%	**0.009**	0.472
gamma-glutamylisoleucine*	26%	2%	56%	**0.034**	31%	7%	59%	**0.010**	28%	5%	56%	**0.018**	0.605
S-lactoylglutathione	-30%	-58%	16%	0.171	-54%	-74%	-18%	**0.011**	-41%	-62%	-10%	**0.019**	0.361
gamma-glutamylcysteine	17%	-4%	42%	0.124	27%	5%	52%	**0.014**	22%	3%	44%	**0.024**	0.441
ophthalmate	38%	3%	85%	**0.036**	34%	-2%	81%	0.069	36%	1%	82%	**0.044**	0.668
N-acetyl-aspartyl-glutamate (NAAG)	22%	2%	45%	**0.034**	16%	-2%	37%	0.083	19%	1%	40%	**0.046**	0.231
S-nitrosoglutathione (GSNO)	-13%	-24%	0%	0.051	-11%	-25%	5%	0.181	-12%	-23%	1%	0.081	0.957
glutamate, gamma-methyl ester	25%	-1%	58%	0.067	11%	-9%	36%	0.309	18%	-3%	43%	0.097	0.285
gamma-glutamylglycine	16%	-4%	41%	0.124	14%	-6%	38%	0.196	15%	-3%	37%	0.112	0.803
N-acetylglutamate	8%	-3%	20%	0.157	8%	-2%	18%	0.142	8%	-2%	18%	0.132	0.918
S-1-pyrroline-5-carboxylate	9%	-16%	41%	0.509	30%	-2%	73%	0.077	19%	-6%	51%	0.155	0.195
pyroglutamine*	-7%	-17%	3%	0.185	-5%	-13%	5%	0.307	-6%	-15%	4%	0.222	0.363
glutathione, reduced (GSH)	-5%	-14%	4%	0.277	-5%	-14%	4%	0.279	-5%	-14%	4%	0.253	0.920
5-oxoproline	5%	-5%	16%	0.385	6%	-4%	17%	0.249	5%	-4%	16%	0.266	0.873
2-hydroxybutyrate/2-hydroxyisobutyrate	-1%	-12%	11%	0.874	-9%	-18%	1%	0.081	-5%	-13%	4%	0.285	0.140
4-hydroxy-nonenal-glutathione	15%	-11%	50%	0.291	9%	-15%	39%	0.513	12%	-11%	40%	0.338	0.889
glutamate	3%	-4%	11%	0.385	3%	-4%	10%	0.475	3%	-4%	10%	0.397	0.753
gamma-aminobutyrate (GABA)	7%	-7%	23%	0.361	4%	-10%	19%	0.598	5%	-8%	20%	0.453	0.421
gamma-glutamylglutamine	-11%	-31%	14%	0.363	-3%	-23%	24%	0.832	-7%	-26%	18%	0.554	0.182
glutamine	2%	-16%	24%	0.862	9%	-8%	29%	0.318	5%	-11%	26%	0.556	0.158

alpha-ketoglutarate	-16%	-36%	9%	0.199	7%	-12%	28%	0.507	-6%	-22%	15%	0.567	0.062
gamma-glutamylphenylalanine	0%	-16%	19%	0.998	9%	-6%	26%	0.276	4%	-10%	20%	0.576	0.266
gamma-glutamyl-epsilon-lysine	-2%	-14%	13%	0.829	8%	-6%	24%	0.282	3%	-10%	17%	0.663	0.093
4-hydroxyglutamate	-4%	-18%	13%	0.641	-2%	-16%	15%	0.823	-3%	-16%	12%	0.706	0.759
glycine	-2%	-10%	7%	0.693	-1%	-8%	6%	0.779	-1%	-8%	6%	0.722	0.770
gamma-carboxyglutamate	-4%	-13%	5%	0.389	1%	-8%	12%	0.806	-2%	-10%	8%	0.734	0.140
cysteinylglycine	-3%	-15%	10%	0.614	-1%	-14%	15%	0.897	-2%	-14%	12%	0.793	0.755
cysteine	-8%	-21%	8%	0.311	5%	-12%	25%	0.597	-2%	-15%	14%	0.825	0.169
carboxyethyl-GABA	4%	-17%	29%	0.761	0%	-20%	25%	0.992	1%	-17%	25%	0.890	0.475
gamma-glutamylglutamate	1%	-10%	13%	0.857	-2%	-14%	10%	0.697	-1%	-10%	10%	0.890	0.555
N-acetylglutamine	-2%	-16%	13%	0.735	4%	-9%	20%	0.554	1%	-12%	16%	0.893	0.178
glutathione, oxidized (GSSG)	4%	-5%	13%	0.422	-3%	-11%	6%	0.455	0%	-8%	9%	0.984	**0.045**

*Percent change per copy of rs10911021 risk (‘C’) allele.

Supplementary Table 3. Pair-wise correlations among metabolites associated with rs10911021.

	γ-glutamyl threonine	γ-glutamyl leucine	γ-glutamyl valine	β-citryl glutamate	γ-glutamyl isoleucine	S-lactoyl glutathione	γ-glutamyl cysteine	Ophthalmate	NAAG
γ-glutamylthreonine		0.80 <0.0001	0.80 <0.0001	0.42 0.0007	0.75 <0.0001	-0.30 0.02	0.57 <0.0001	0.68 <0.0001	0.07 NS
γ-glutamylleucine	0.90 <0.0001		0.95 <0.0001	0.30 0.02	0.96 <0.0001	-0.16 NS	0.42 0.0008	0.75 <0.0001	0.07 NS
γ-glutamylvaline	0.89 <0.0001	0.96 <0.0001		0.29 0.02	0.92 <0.0001	-0.17 NS	0.42 0.0008	0.77 <0.0001	0.01 NS
β-citrylglutamate	0.39 0.002	0.36 0.005	0.35 0.006		0.26 0.04	-0.33 0.008	0.61 <0.0001	0.19 NS	0.40 0.001
γ-glutamylisoleucine	0.85 <0.0001	0.97 <0.0001	0.95 <0.0001	0.30 0.02		-0.14 NS	0.32 0.01	0.70 <0.0001	0.04 NS
S-lactoylglutathione	-0.15 NS	-0.19 NS	-0.14 NS	-0.33 0.009	-0.13 NS		-0.39 0.002	-0.15 NS	-0.26 0.04
γ-glutamylcysteine	0.65 <0.0001	0.59 <0.0001	0.54 <0.0001	0.58 <0.0001	0.47 <0.0001	-0.49 <0.0001		0.39 0.002	0.29 0.02
ophthalmate	0.78 <0.0001	0.80 <0.0001	0.84 <0.0001	0.22 NS	0.80 <0.0001	0.04 NS	0.32 0.01		0.04 NS
N-acetyl-aspartyl-glutamate (NAAG)	0.08 NS	0.05 NS	-0.02 NS	0.51 <0.0001	0.01 NS	-0.28 0.03	0.26 0.05	0.01 NS	

Values are Pearson correlation coefficients (upper line) and the corresponding p values (lower line).
Correlations above and below the diagonal refer to low and high glucose, respectively.

Supplementary Table 4. Correlation between metabolites associated with rs10911021 and glutamate, glutamine, GSH, and GSH/glutamate ratio.

	5 mM glucose					25 mM glucose			
	Glutamate	Glutamine	GSH	GSH/ glutamate		Glutamate	Glutamine	GSH	GSH/ glutamate
γ-glutamylthreonine	0.46 0.0002	0.15 NS	-0.08 NS	-0.50 P<0.0001		0.25 0.048	0.19 NS	-0.29 0.02	-0.61 <0.0001
γ-glutamylleucine	0.38 0.002	0.11 NS	-0.25 0.05	-0.62 P<0.0001		0.26 0.0438	0.22 0.09	-0.30 0.02	-0.63 <0.0001
γ-glutamylvaline	0.36 0.004	0.09 NS	-0.26 0.04	-0.62 P<0.0001		0.25 0.0532	0.25 0.05	-0.29 0.02	-0.61 <0.0001
β-citrylglutamate	0.66 <0.0001	0.30 0.02	0.43 0.0004	-0.06 NS		0.64 <0.0001	0.36 0.004	0.38 0.002	-0.11 NS
γ-glutamylisoleucine	0.36 0.004	0.16 NS	-0.27 0.03	-0.63 <0.0001		0.20 0.1155	0.24 0.06	-0.34 0.006	-0.63 <0.0001
S-lactoylglutathione	-0.20 NS	-0.06 NS	-0.04 NS	0.13 NS		-0.32 0.01	-0.20 NS	-0.17 NS	0.07 NS
γ-glutamylcysteine	0.62 <0.0001	0.08 NS	0.42 0.0006	-0.04 NS		0.53 <.00001	0.11 NS	0.26 0.04	-0.17 NS
ophthalmate	0.20 NS	0.11 NS	-0.25 0.05	-0.47 0.0001		0.04 NS	0.18 NS	-0.38 0.002	-0.53 <0.0001
N-acetyl-aspartyl-glutamate (NAAG)	0.20 NS	-0.08 NS	0.1 NS	-0.05 NS		0.19 NS	0.02 NS	0.12 NS	-0.02 NS

Supplementary Figure 1. Intracellular levels of glutamate, glutamine, and reduced glutathione in relation to rs10911021 genotype. No association between these metabolites and rs1091102 was observed in either low or high glucose.

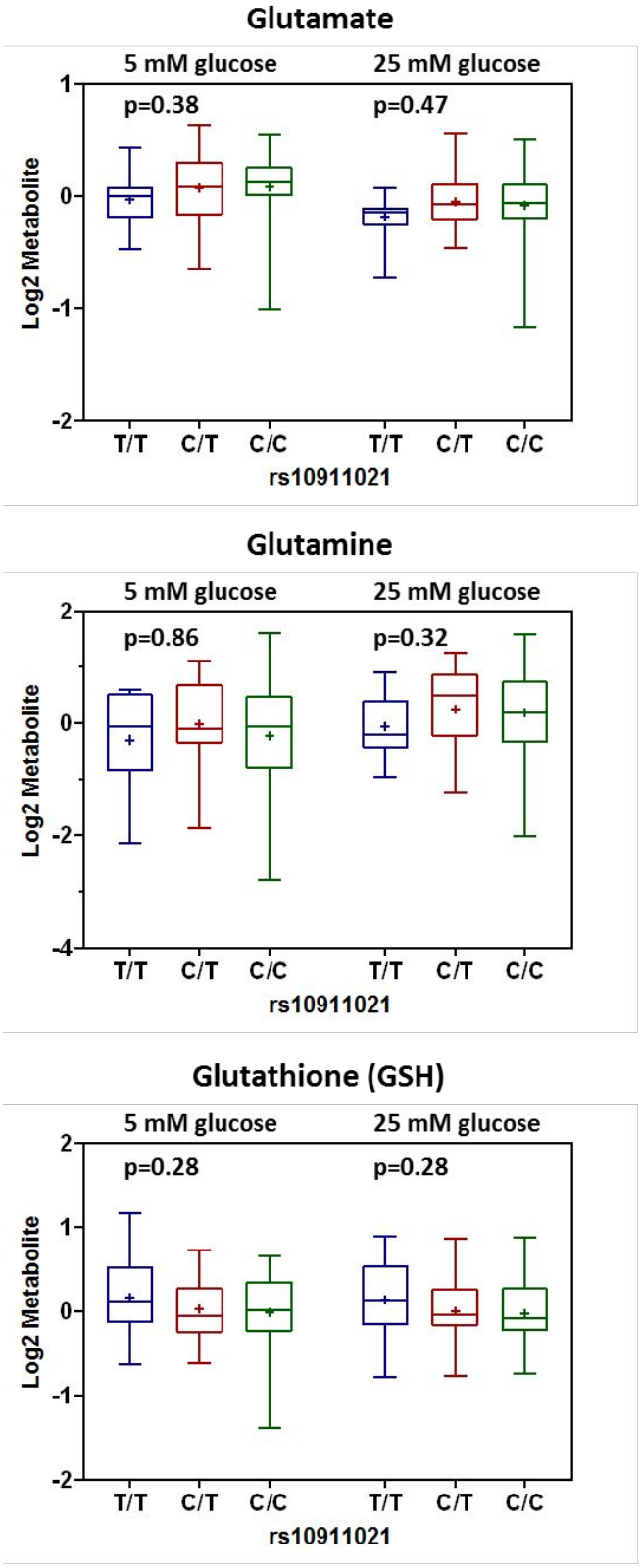

Supplementary Figure 2. Intracellular levels of oxidized tyrosines. 3-chloro-tyrosine levels were significantly associated with the rs10911021 genotype in 25 mM glucose (p=0.02). No association with the genotype was detected for 3-nitro-tyrosine and o',o'dityrosine in either low or high glucose.